

Thrombus Volume Change Visualization after Endovascular Abdominal Aortic Aneurysm Repair

Josu Maiora^{1,4}, Guillermo García², Iván Macía^{3,4}, Jon Haitz Legarreta³, Fernando Boto³, Céline Paloc³, Manuel Graña⁴ and Javier Sanchez Abuín⁵,

¹ Electronics and Telecommunications Department, ² Engineering Systems and Automatic Department, Technical University School, University of the Basque Country, Donostia-San Sebastián, Spain
{j.maiora, g.garcia}@ehu.es

³ eHealth and Biomedical Applications Department, Vicomtech, Donostia-San Sebastián, Spain
{imacia, jhlegarreta, fboto, cpaloc}@vicomtech.org

⁴ Computational Intelligence Group, Computer Science Faculty, University of the Basque Country, Donostia-SanSebastián, Spain
manuel.grana@ehu.es

⁵ Interventional Radiology Service, Donostia Hospital, Donostia-SanSebastián, Spain
javier.sanchezabuin@osakidetza.net

Abstract. A surgical technique currently used in the treatment of Abdominal Aortic Aneurysms (AAA) is the Endovascular Aneurysm Repair (EVAR). This minimally invasive procedure involves inserting a prosthesis in the aortic vessel that excludes the aneurysm from the bloodstream. The stent, once in place acts as a false lumen for the blood current to travel down, and not into the surrounding aneurysm sac. This procedure, therefore, immediately takes the pressure off the aneurysm, which thromboses itself after some time. Nevertheless, in a long term perspective, different complications such as prosthesis displacement or bloodstream leaks into or from the aneurysmatic bulge (endoleaks) could appear causing a pressure elevation and, as a result, increasing the danger of rupture. The purpose of this work is to explore the application of image registration techniques to the visual detection of changes in the thrombus in order to assess the evolution of the aneurysm. Prior to registration, both the lumen and the thrombus are segmented

1 Introduction

Abdominal Aortic Aneurysms (AAA) [1, 2] are a focal dilation in some point of the abdominal section of the aorta. Several treatments exist today; one option is a minimally invasive surgical procedure called Endovascular Aneurysm Repair

(EVAR) in which an endovascular prosthesis (endovascular graft) is inserted to exclude the aneurysm from blood circulation [3].

The EVAR (Fig.1) requires a postoperative follow-up to ensure that the stent is stable (absence of leakage, i.e.: blood flow within the aneurysm's sack). A reduction in the size of the aneurysm ensures that exclusion has been effective [4, 5], while an expansion and/or the presence of a leakage are indicators that the treatment has not been effective, maintaining the risk of blood vessel rupture at the aneurysm location.

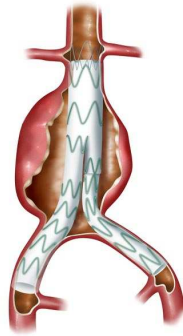


Fig. 1. Endovascular graft

The most widely used technique for EVAR monitoring is to obtain Computerized Tomography (CT) images of the abdominal region after an intravenous contrast agent has been injected. Such scans of the patient's abdominal area are available in the clinical routine as a set of 2D images whose visual analysis is time-consuming. The aim of our work is to make an automatic analysis of the AAA using digital image processing techniques, and yielding visual and quantitative information for monitoring and tracking of patients who underwent EVAR.

In our approach, first we estimate the rigid motion of the stent, as well as its deformation [6], and then we compute the spatial transformation of the segmented thrombus according to this estimation. Visual overlapping of such transformed data can help identifying deformation patterns having a high probability of dangerous progression of the aneurysm. The long term goal of our research is to make a prediction about future complications and disease progression. In the current state of the art of EVAR monitoring, the morphological changes and migration of the thrombus after EVAR are not studied in a systematic manner. The following are the main advances of our work concerning this state of the art:

- We use semi-automatic segmentation methods to segment the aneurysm lumen and thrombus. Using semi-automatic methods make the segmentation process less dependent on the intra-rater and intra-rater variability, that have a proven intra-rater and interrater reliability and validity. A novel technique for thrombus segmentation, based on region growing algorithms, centerline extraction and radial functions, is used.

- Current registration methods used in EVAR monitoring are based in point set registration methods, which suffer from information loss. In our processing pipeline, registration is performed over binary images with much less information loss.

The processing pipeline is illustrated in figure 2. We compute the registration of the lumen of the last image to the target image. This registration allows aligning the two images to the same reference system. We compute a sequence of rigid, affine and deformable registrations, and then we apply the obtained lumen transformation to the thrombus.

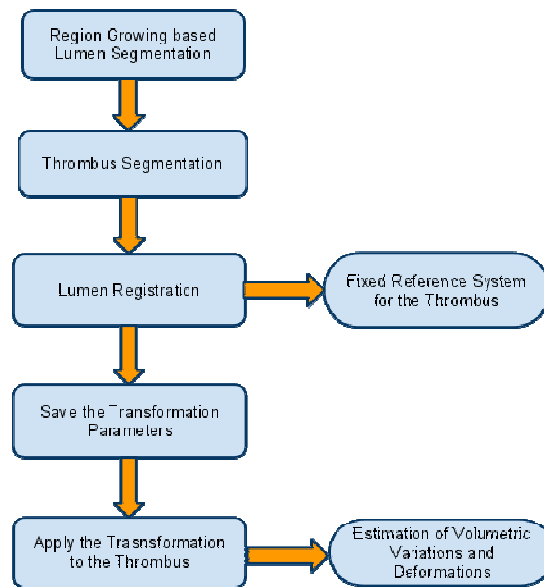


Fig. 2. Pipeline of the thrombus visual change detection process

2 Methods

We estimate the volumetric variations, as well as the deformations of the thrombus in a patient, (across different studies), registering the lumen of the aorta of the datasets to be compared, in order to place the respective thrombi in the same reference system, so that the comparison becomes meaningful. This registration is necessary because the relative position of the aorta varies from different studies of the same patient along time.

First, the lumen is segmented using a 3D region growing algorithm, followed by the calculation of the aorta centerline. The thrombus is segmented using a radial model approach [7]. After that, the registration of the lumen extracted from two datasets of the same patient obtained at different moments in time is computed and

then, the obtained transformation is applied to the thrombus. Next, we proceed to describe each component of the system.

2.1 Image Segmentation

The first step in image analysis generally is to segment the image. Segmentation subdivides an image into its constituent parts or objects, which are defined as homogenous and disjoint regions (image segments) that are separated by boundaries. Independent of the segmentation technique, images usually need to be preprocessed for efficient segmentation[7].

Region Growing based Lumen Segmentation

Segmentation of the lumen is based on a 3D region-growing algorithm that needs an interactive selection of a seed voxel. First, the image is preprocessed to reduce noise and a Volume of Interest (VOI) is defined in order to reduce the data amount to be processed. The algorithm includes voxels whose intensity lies in the confidence interval of the intensity of the current segmented region in an iterative process that recomputes the region statistics at each iteration. The segmentation is smoothed by morphological closing of the resulting segmented region to fill possible small holes.

Centerline Extraction

The centerline approximates at each slice the centroid of the lumen region and is a good approximation for the morphological skeleton of the whole aorta. A single point on the center-line is obtained for every slice, since the aorta is almost normal to axial slices. The center-line determination is performed on a slice-by-slice basis using 2D image moments.

Thrombus Segmentation

We propose modeling the internal and external contours of the thrombus of the aneurysm as radial functions in cylindrical coordinates. At every slice, we choose the origin of these functions to be the centerline point of this slice. The segmentation procedure consists of calculating the internal and external radii at every point, which enclose the segmented region corresponding to the thrombus.

2.2 Image registration

A spatial transformation maps each point in the 3D space to another point in the same space. Appropriate interpolator, cost/error function and an optimization methods are chosen to compute the optimal adjustment of the transformation parameters corresponding to a minimum of the cost function [8].

2.2.1 Lumen Registration

Our problem is an intra-subject and mono-modal registration, as it examines the same patient on different dates. A sequence of rigid, affine and deformable (B-splines) registrations is performed. The earliest CT volume is considered the target image and the others are registered according to it. A linear interpolator, Squared Intensity Differences and Mutual Information metrics and Regular Step Gradient Descent Optimizer are used to obtain the optimal transformation parameters.

Rigid Registration

First the two binary images corresponding to the patient's lumen are roughly aligned by using a transform initialization. Then the two images are registered using a rigid transformation. In three dimensions we have 6 degrees of freedom, which can be defined as translations in the x , y and z directions, and rotations α , β and γ around these three axes. From these unknowns we can construct a rigid body transformation matrix T_{rigid} . This transformation can be presented as a rotation R followed by a translation t that can be applied to any point x in the image domain.

$$T_{rigid}(x) = Rx + t$$

Affine Registration

The rigid transformation is used to initialize a registration with an affine transform of the lumen. While a rigid transformation preserves the distances between all points in the object transformed, an affine transformation preserves parallel lines. This model has 12 degrees of freedom and allows for scaling and shearing.

$$T(x, y, z) = \begin{pmatrix} x' \\ y' \\ z' \\ 1 \end{pmatrix} = \begin{pmatrix} a_{00} & a_{01} & a_{02} & a_{03} \\ a_{10} & a_{11} & a_{12} & a_{13} \\ a_{20} & a_{21} & a_{22} & a_{23} \\ 0 & 0 & 0 & 1 \end{pmatrix} \begin{pmatrix} x \\ y \\ z \\ 1 \end{pmatrix}$$

Deformable Registration

The warped image resulting from the affine registration is used as the initial image of a B-spline deformable transformation. Free Form Deformations (FFDs) based in locally controlled functions such as B-splines are a powerful tool for modelling 3D deformable objects. We use FFDs is to deform the lumen by manipulating an underlying mesh of control points. The resulting deformation controls the shape of the lumen and produces a smooth and continuous transformation. A spline-based FFD is defined on the image domain $\Omega = \{(x, y, z) | 0 \leq x < X, 0 \leq y < Y, 0 \leq z < Z\}$ where Φ denotes an $n_x \times n_y \times n_z$ mesh of control points $\phi_{i,j,k}$ with uniform spacing δ . In this case, the displacement field \mathbf{u} defined by FFD can be expressed as the 3D tensor product of the 1D cubic B-splines:

$$\mathbf{u}(x, y, z) = \sum_{l=0}^3 \sum_{m=0}^3 \sum_{n=0}^3 \theta(u)\theta(v)\theta(w)\phi_{i+l,j+m,k+n}$$

2.2.2 Evaluation of the registration quality

We use two similarity metrics: the sum of squared intensity differences (SSD) and mutual information (MI). These similarity metrics have each been used widely in the literature for non-rigid registration to measure the intensity agreement between a warped image and the target image. We briefly describe both distances in this section, following [9, 10].

SSD is suitable when the images have been acquired through similar sensors and thus are expected to present the same intensity range and distribution. For voxel locations x_A in image A, within an overlap domain $\Omega_{A,B}^T$, comprising N voxels:

$$SSD = \frac{1}{N} \sum_{x_A \in \Omega_{A,B}^T} |A(x_A) - B^T(x_A)|^2$$

where B^T is the transformed image.

Mutual information is a measure of how much information one random variable has about another. The information contributed by the images is simply the entropy of the portion of the image that overlaps with the other image volume, and the mutual information is a measure of the joint entropy with regard to the marginal entropies.

$$I(A, B) = H(A) + H(B) - H(A, B)$$

where $I(A, B)$ is the mutual information, $H(A)$ and $H(B)$ are the marginal entropies of the target and warped images and $H(A, B)$ is the joint entropy.

3 Results

We have tested the approach with 3 patients –with 5 datasets each– which have been treated with stent-graft devices. The CT image stacks consists of datasets obtained from a LightSpeed16 CT scanner (GE Medical Systems, Fairfield, CT, USA) with 512x512x354 voxel resolution and 0.725x0.725x0.8 mm. spatial resolution. The time elapsed between different studies of the same subject varies between 6 and 12 months.

We have computed the mean squares and mutual information similarity metrics for the evaluation of the registration. A decrease of both metric is observed in the consequent registration methods. Mutual information is reported as a negative number because it has been used as a cost function by the minimization algorithm.

Table 1. Similarity metric results of the sequence of registrations over one of the patient datasets. Image 2 is the target image for registration of images 3, 4 and 5.

Registered Studies		Metrics	
		Mean Squares	Mutual Information
2-3	Rigid	4,60E-01	-5,28E-06
	Affine	3,42E-01	-7,25E-06
	Deform. Coarse	3,05E-01	-8,35E-06
	Deform. Fine	2,88E-01	-9,24E-06
2-4	Rigid	4,94E-01	-4,96E-06
	Affine	2,97E-01	-7,91E-06
	Deform. Coarse	2,70E-01	-8,64E-06
	Deform. Fine	2,65E-01	-9,53E-06
2-5	Rigid	8,03E-01	-3,48E-06
	Affine	3,73E-01	-6,29E-06
	Deform. Coarse	3,19E-01	-7,27E-06
	Deform. Fine	2,88E-01	-8,96E-06

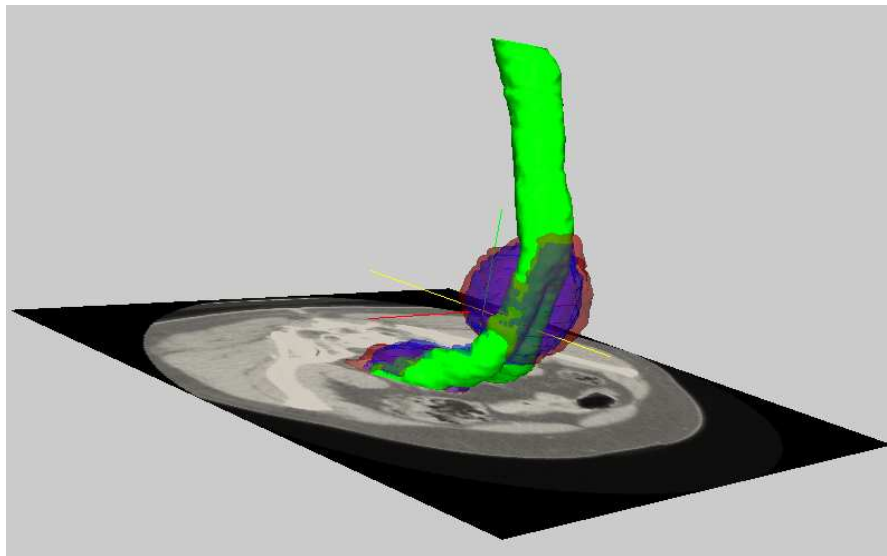


Fig. 3. Thrombus extracted for two instants in time (semi-transparent blue for the first one, semi-transparent red the second one), both registered to the lumen of the first instant in time. An increase in thrombus volume can be easily appreciated

The segmented images are visualized in 3D together with a CT slice to have a referenced view. After the lumen is registered, volumetric changes and deformation of the thrombus from one point in time to the next can be visualized (Fig. 3).

4 Conclusion

We have developed a method that places the thrombi of different datasets of the same patient referenced to the lumen of the first dataset. The method allows detecting small changes in volume or deformation of the thrombus that may go unnoticed for radiologists while comparing individual slices of the same patient along time. With our method, any change in volume can be detected easily.

In the future, we expect to obtain quantitative values of the changes in the thrombus after registration of images from different studies of the same patient. This could lead to a model that could predict the evolution of other patients and provide quantitative measurements for decision support. Support Vector Machines (SVM) will be used to determine if the evolution of the EVAR is positive or not.

References

- 1 J.Cronenwett, W.Krupski, and R.Rutherford: 'Abdominal aortic and iliac aneurysm'. Saunders, Philadelphia. Vascular Surgery, pp. 1246-1280 (2000).
- 2 Rodin, M.B., Daviglius, M.L., Wong, G.C., Liu, K., Garside, D.B., Greenland, P., and Stamler, J.: 'Middle age cardiovascular risk factors and abdominal aortic aneurysm in older age', *Hypertension*, 2003, 42, (1), pp. 61-68
- 3 Veith, F.J., Marin, M.L., Cynamon, J., Schonholz, C., and Parodi, J.: '1992: Parodi, Montefiore, and the first abdominal aortic aneurysm stent graft in the United States', *Annals of Vascular Surgery*, 2005, 19, (5), pp. 749-751
- 4 Ellozy, S.H., Carroccio, A., Lookstein, R.A., Jacobs, T.S., Addis, M.D., Teodorescu, V.J., and Marin, M.L.: 'Abdominal aortic aneurysm sac shrinkage after endovascular aneurysm repair: Correlation with chronic sac pressure measurement', *Journal of Vascular Surgery*, 2006, 43, (1), pp. 2-6
- 5 Dias, N.V., Ivancev, K., Malina, M., Resch, T., Lindblad, B., and Sonesson, B.: 'Intra-aneurysm sac pressure measurements after endovascular aneurysm repair: Differences between shrinking, unchanged, and expanding aneurysms with and without endoleaks', *Journal of Vascular Surgery*, 2004, 39, (6), pp. 1229-1235
- 6 Mattes, J., Steingruber, I., Netzer, M., Fritscher, K., Kopf, H., Jaschke, W., and Schubert, R.: 'Quantification of the migration and deformation of abdominal aortic aneurysm stent grafts - art. no. 61440V', in Reinhardt, J.M., and Pluim, J.P.W. (Eds.): 'Medical Imaging 2006: Image Processing, Pts 1-3' (2006), pp. V1440-V1440
- 7 M. Garcia-Sebastian, A. I. Gonzalez, and M. Grana, 'An adaptive field rule for non-parametric MRI intensity inhomogeneity estimation algorithm', *Neurocomputing*, vol. 72, no. 16-18, pp. 3556-3569, 2009.
- 8 Macía, I., Legarreta, J.H., Paloc, C., Graña, M., Maiora, J., García, G., de Blas, M.: Segmentation of Abdominal Aortic Aneurysms in CT Images using a Radial Model Approach. LNCS, vol. 5788, pp. 664--671. Springer Verlag, Heidelberg (2009).
- 9 Ibanez, L., Ng, L., Gee, J., Aylward, S.: 'Registration patterns: The generic framework for image registration of the insight toolkit' 2002 Ieee International Symposium on Biomedical Imaging, Proceedings (2002)
- 10 Yanovsky, I., Leow, A.D., Lee, S., Osher, S.J., and Thompson, P.M.: 'Comparing registration methods for mapping brain change using tensor-based morphometry', *Medical Image Analysis*, 2009, 13, (5), pp. 679-700